Medical Engineering & Physics 32 (2010) 584–594

Contents lists available at ScienceDirect

Medical Engineering & Physics

journal homepage: www.elsevier.com/locate/medengphy

Surrogate articular contact models for computationally efficient multibody dynamic simulations

Yi-Chung Lin [a], Raphael T. Haftka [a], Nestor V. Queipo [b], Benjamin J. Fregly [a,c,d,*]

[a] Department of Mechanical & Aerospace Engineering, University of Florida, Gainesville, FL, USA
[b] Applied Computing Institute, University of Zulia, Maracaibo, Venezuela
[c] Department of Biomedical Engineering, University of Florida, Gainesville, FL, USA
[d] Department of Orthopaedics and Rehabilitation, University of Florida, Gainesville, FL, USA

ARTICLE INFO

Article history:
Received 16 July 2009
Received in revised form 8 February 2010
Accepted 10 February 2010

Keywords:
Elastic contact
Surrogate modeling
Multibody dynamics
Biomechanics

ABSTRACT

Contact occurs in a wide variety of multibody dynamic systems, including the human musculoskeletal system. However, sensitivity and optimization studies of such systems have been limited by the high computational cost of repeated contact analyses. This study presents a novel surrogate modeling approach for performing computationally efficient three-dimensional elastic contact analyses within multibody dynamic simulations. The approach fits a computationally cheap surrogate contact model to data points sampled from a computationally expensive elastic contact model (e.g., a finite element or elastic foundation model) and resolves several unique challenges involved in applying surrogate modeling techniques to elastic contact problems. As an example application, we performed multibody dynamic simulations of a Stanmore wear simulator machine using surrogate and elastic foundation (EF) contact models of a total knee replacement. Accuracy was assessed by performing eleven dynamic simulations with both types of contact models utilizing large variations in motion and load inputs to the machine. Wear volumes predicted with the surrogate contact models were within 1.5% of those predicted with the EF contact models. Computational speed was assessed by performing five Monte Carlo analyses (over 1000 dynamic simulations each) with surrogate contact models utilizing realistic variations in motion and load inputs. Computation time was reduced from an estimated 284 h per analysis with the EF contact models to 1.4 h with the surrogate contact models (i.e., 17 min vs. 5 s per simulation), with higher wear sensitivity observed for motion variations than for load variations. The proposed surrogate modeling approach can significantly improve the computational speed of multibody dynamic simulations incorporating three-dimensional elastic contact models with general surface geometry.

1. Introduction

Multibody dynamic simulation of systems experiencing contact is valuable for engineering applications ranging from the design of industrial machines and mechanisms to the analysis of human joints. Computational contact models used to perform such simulations generally fall into two categories: rigid or deformable [1,2]. Rigid body contact models use unilateral constraints to maintain contact between opposing surfaces and are highly efficient computationally for predicting motion [3]. However, they do not permit calculation of unique contact forces under statically indeterminate conditions, such as when contact occurs in two or more places between the same pair of contacting bodies [4]. Furthermore, they often require different computational schemes to simulate continuous contact versus intermittent impact.

In contrast, deformable body contact models, such as finite element models [5–14] and elastic foundation models [15–22], provide a unified approach for simulating continuous contact versus intermittent impact, and they can calculate unique contact forces in statically indeterminate situations. Furthermore, they permit calculation of contact pressures and strains across the opposing surfaces. Unfortunately, the high computational cost of deformable body contact analyses, particularly due to extensive repeated geometry evaluations, significantly limits their use in multibody dynamic simulations [16,20]. Thus, no contact modeling approach currently exists that provides the functional benefits of deformable body contact methods along with the computational speed of rigid body contact methods.

In other engineering disciplines, surrogate modeling approaches have been used successfully to overcome similar computational challenges [23–29]. These approaches replace a computationally costly original model (e.g., a finite element model) with a com-

* Corresponding author at: Department of Mechanical & Aerospace Engineering, 231 MAE-A Building, PO Box 116250, University of Florida, Gainesville, FL 32611-6250, USA. Tel.: +1 352 392 8157; fax: +1 352 392 7303.
E-mail address: fregly@ufl.edu (B.J. Fregly).

1350-4533/$ – see front matter © 2010 IPEM. Published by Elsevier Ltd. All rights reserved.
doi:10.1016/j.medengphy.2010.02.008

putationally cheap surrogate model fitted to data points sampled from the original model. Once constructed, the surrogate model is used in place of the original model to eliminate computational bottlenecks. Only a small number of studies have applied surrogate modeling techniques to contact problems [30–34]. However, none of these studies have addressed how surrogate contact modeling approaches can be applied to three-dimensional (3D) multibody dynamic simulations. In particular, no study has resolved how sampling should be performed, since many sample point combinations will result in physically undesirable situations where the contacting bodies are either out of contact or deeply penetrating.

This study proposes a novel method for performing computationally efficient 3D elastic contact analyses within multibody dynamic simulations, thereby eliminating contact analyses as a computational bottleneck. The method is based on surrogate modeling techniques augmented with two key concepts – "sensitive directions" and a "reasonable design space" [27] – to address the unique challenges posed by elastic contact problems. The accuracy and computational speed of the method are evaluated by performing thousands of multibody dynamic wear simulations for a total knee replacement (TKR) design tested in a Stanmore knee simulator machine.

2. Methods

2.1. Surrogate contact model concepts

The 10 concepts listed below provide the foundation for creating a surrogate contact model that can calculate contact loads (and possibly other quantities of interest) for a single contact occurring between a single pair of bodies:

(1) A three-dimensional frictionless elastic contact model (i.e., the "original model") is the computationally costly model to be replaced with a computationally cheap surrogate model.
(2) One of the contacting bodies is treated as the master body and the other as the slave body, where both bodies possess general surface geometry and material properties.
(3) The pose of the slave body relative to the master body is defined by six pose parameters (i.e., three translations x, y, z along with three rotations α, β, γ using a specified rotation sequence).
(4) For each combination of six pose parameters there exists a unique combination of six contact loads (i.e., three forces F_x, F_y, F_z and three torques T_α, T_β, T_γ) applied to the two contacting bodies in an equal and opposite sense.
(5) For any pose, each contact load is most sensitive to changes in the corresponding pose parameter (e.g., F_y is most sensitive to changes in y).
(6) A "sample point" is any combination of six pose and load inputs to the original model (e.g., x, F_y, z, α, β, γ) for which the six corresponding load and pose outputs are desired (e.g., F_x, y, F_z, T_α, T_β, T_γ).
(7) A sample point is labeled as "desirable" when it produces contact load and pose outputs that are all within some pre-defined bounds. If any load or pose output is outside the pre-defined bounds, the sample point is labeled as "undesirable."
(8) Given a large number of sample points, repeated static analyses can be performed with the original model to generate input–output relationships to be fitted by the surrogate model.
(9) A surrogate contact model is actually a collection of six separate surrogate models – one for each of the six contact loads as a function of the six pose parameters.
(10) Quantities other than contact loads can also be fitted as surrogate model outputs (e.g., maximum and average contact pressure, contact area, center of pressure location).

2.2. Surrogate contact model development

Application of surrogate modeling techniques to 3D elastic contact problems poses a number of unique challenges. To address these challenges, which are described in the current section, we have developed special surrogate model creation methods. These methods are based on the ten concepts listed in the previous section and are organized into a five-step process.

2.2.1. Step (1): identify sensitive and insensitive directions in the original contact model

The surrogate model creation process involves performing repeated computational experiments with the original contact model to generate input–output pairs to be fitted by the surrogate contact model. The combinations of inputs to be analyzed are selected using design of experiments (DOE), which employs statistical methods to scatter sample points uniformly throughout a bounded six-dimensional design space. Within the context of a multibody dynamic simulation, the desired inputs to a 3D elastic contact model are the six pose parameters and the desired outputs are the six contact loads [16]. Thus, using a traditional DOE sampling method, sample points would be combinations of the six pose parameters x, y, z, α, β, γ, with an upper and lower bound placed on each one. The problem with this approach is that physically realistic contact occurs over a thin hypersurface in six-dimensional pose parameter design space. Consequently, many of the selected sample points will correspond to situations where the opposing surfaces are either out of contact or deeply interpenetrating. These situations are problematic since inclusion of physically unrealistic sample points reduces the accuracy of the resulting surrogate contact model.

To develop a method for resolving this issue, we propose the concept of "sensitive directions." When the master and slave body are in contact, some contact loads will be highly sensitive to changes in their corresponding pose parameters, while others will be insensitive. To quantify these sensitivities, we calculate six finite-difference derivatives and collect the results in a sensitivity vector $\mathbf{s}$:

$$\mathbf{s} = \left[\frac{\partial F_x}{\partial x} \quad \frac{\partial F_y}{\partial y} \quad \frac{\partial F_z}{\partial z} \quad \frac{\partial T_\alpha}{\partial \alpha} \quad \frac{\partial T_\beta}{\partial \beta} \quad \frac{\partial T_\gamma}{\partial \gamma} \right] \tag{1}$$

A direction for which a contact force or torque is sensitive to changes in the corresponding pose parameter is termed a "sensitive direction," and the remaining directions are termed "insensitive directions." Due to differences in units, sensitive directions are evaluated separately for translations (first three entries of $\mathbf{s}$) and rotations (last three entries of $\mathbf{s}$). If one translational (or rotational) derivative in $\mathbf{s}$ is significantly larger than the other two, the corresponding direction is deemed a sensitive direction. If two translational (or rotational) derivatives are significantly larger than the third, then two sensitive directions exist. For some situations (e.g., conformal contact between a sphere and a spherical cup of slightly larger radius), all three translational (or rotational) derivatives may be of comparable magnitude, in which case knowledge of the physical situation must be used to determine whether three or zero sensitive directions exist. At least one translational sensitive direction will always exist corresponding to an approximate contact normal direction, and two or more sensitive directions may exist depending on the geometry of the contacting bodies.

2.2.2. Step (2): avoid sample points with undesirable contact load outputs in sensitive directions by changing the definition of a sample point

Once sensitive directions have been identified, we modify the definition of a sample point such that pose parameters for sensitive directions are replaced by their corresponding contact loads. For example, if y is identified as a sensitive direction, then y would be replaced with F_y in the sample point definition. With this non-traditional sampling method, sample points become combinations of pose parameters and contact loads (e.g., x, F_y, z, α, β, γ), with an upper and lower bound placed on each input.

For sampling of the original contact model, use of contact loads as inputs for sensitive directions has two important consequences. First, contact load outputs from the original contact model in the sensitive directions will be guaranteed to be within their specified bounds (i.e., no zero or excessively high contact loads). Second, inputs to the original contact model during sampling (i.e., a combination of pose parameters and loads) will now be different from inputs to the surrogate contact model during a multibody dynamic simulation (i.e., pose parameters only). This second consequence will influence the fifth step of the surrogate contact model creation process.

2.2.3. Step (3): generate sample point input–output pairs by using design of experiments and repeated static analyses

Given this modified sample point definition, we generate a specified number of sample points n using a traditional DOE approach. Common approaches include optimal Latin hypercube sampling [35], Hammersley quasirandom (HQ) sampling [36], and face-centered central composite design [37]. We choose to use HQ sampling for three reasons. First, HQ sampling provides better uniformity properties than do other sampling techniques for sample points generated within a multi-dimensional hypercube [38,39]. Second, HQ sample points are generated sequentially rather than simultaneously. Thus, the first m sample points from a larger set of n sample points ($n > m$) will always be approximately equidistant from one another and can be used as a subsample. Third, all existing sample points can be kept if new sample points need to be added.

To evaluate a sample point, we perform a static analysis with the original contact model. During the analysis, sensitive directions are left free to equilibrate under the applied loads, while insensitive directions are constrained to the specified pose parameter values. Once the static configuration is reached, the resulting contact loads in the sensitive directions are compared to the corresponding applied loads. If any difference is above 0.1% (i.e., the final static configuration is not truly static), the sample point is deemed to be undesirable and is discarded.

2.2.4. Step (4): eliminate sample points with undesirable contact load outputs in insensitive directions by using the concept of a reasonable design space

While changing the definition of a sample point avoids undesirable contact load outputs for sensitive directions, undesirable contact load outputs for insensitive directions can still occur. Putting bounds on contact load outputs for insensitive directions provides an additional avenue for narrowing the sample point envelope, thereby improving surrogate model accuracy. Thus, in addition to placing physically realistic upper and lower bounds on the pose parameter and contact load inputs (e.g., x, F_y, z, α, β, γ), we also place physically realistic upper and lower bounds on the corresponding contact load (and if desired, pose parameter) outputs (e.g., F_x, y, F_z, T_α, T_β, T_γ). These bounds are estimated by performing one or more nominal dynamic simulations with the original contact model and expanding the observed range of each contact load output by some specified percentage p. The resulting range for the outputs is termed the "reasonable design space" [27,40,41]. Sample points whose contact load outputs are outside the reasonable design space are deemed undesirable and are discarded.

Evaluation of undesirable sample points by the original contact model would waste a large amount of CPU time performing computationally costly static analyses whose results would be discarded. To address this problem, we use an initial coarse surrogate contact model to eliminate undesirable sample points [42]. This model is constructed from a subset m of the complete set of n sample points generated by HQ sampling. These m sample points are then evaluated in a three-step subprocess. First, a static analysis is performed with the original contact model for each of the m sample points, and undesirable sample points are identified and eliminated. Second, a coarse surrogate contact model is created by fitting each of the six static analysis outputs (e.g., F_x, y, F_z, T_α, T_β, T_γ) for the remaining points ($<m$) as functions of the six static analysis inputs (e.g., x, F_y, z, α, β, γ). Fitting is performed using Kriging [43], a multi-dimensional non-uniform interpolation method, since our preliminary studies revealed that Kriging produces more accurate dynamic simulation results than do a variety of other surrogate model fitting methods (e.g., polynomial response surfaces and support vector regression). Third, the coarse surrogate model is evaluated repeatedly to estimate the outputs for the remaining $n–m$ sample points. Since a large number of the $n–m$ sample points contain undesirable contact load outputs, screening these points with the coarse surrogate contact model provides significant computational savings during surrogate model construction.

2.2.5. Step (5): construct the final surrogate contact model using the desirable subset of the original sample points

Fitting the final surrogate contact model to the desirable subset of sample points is complicated by the fact that contact model inputs and outputs are different for sampling versus use in a dynamic simulation. To illustrate this issue, we consider an elastic contact model whose only sensitive direction is y translation. During sampling, inputs to the original contact model would be x, F_y, z, α, β, γ while outputs would be F_x, y, F_z, T_α, T_β, T_γ. In contrast, during a multibody dynamic simulation, inputs to the surrogate contact model would be x, y, z, α, β, γ while outputs would be F_x, F_y, F_z, T_α, T_β, T_γ. This slight change in input and output definitions is problematic since in pose parameter space, the reasonable design space is thin and curved, making the fitting process ill conditioned. The alternative is to calculate contact loads in sensitive directions by solving a nonlinear root-finding problem (e.g., given x, y, z, α, β, γ, find F_y by solving $f(x, F_y, z, \alpha, \beta, \gamma) - y = 0$.

With this issue in mind, the final surrogate contact model is created as follows. Repeated static analyses are performed with the original contact model for all desirable sample points not yet evaluated. Since these sample points were retained based on initial surrogate contact model predictions, some of them will have outputs that are outside the reasonable design space and will be discarded. The remaining set of desirable sample points ($\ll n$) is used to construct the final surrogate contact model, again using Kriging. Contact loads corresponding to sensitive directions are fitted as a function of the six pose parameters (e.g., $F_y = f(x, y, z, \alpha, \beta, \gamma)$), while contact loads corresponding to insensitive directions are fitted as a function of contact loads in sensitive directions and pose parameters in insensitive ones (e.g., $F_x = f(x, F_y, z, \alpha, \beta, \gamma)$). This approach eliminates the problem of ill-conditioned fitting as well as the need to solve a nonlinear root-finding problem for the sensitive directions. Once a Kriging-based surrogate contact model has been constructed, it is used to calculate six contact loads at each time instant during a dynamic simulation given the six pose parameters for the contacting bodies.

While the surrogate contact modeling approach described above assumes that only a single contact occurs between each pair of contacting bodies and that contact loads are the only desired

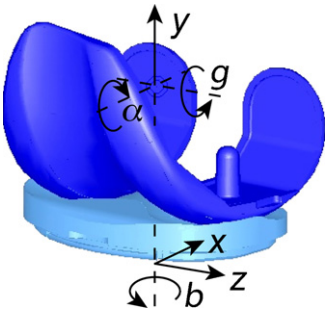

Fig. 1. Multibody dynamic model of a commercial knee implant in a Stanmore knee simulator machine. The tibial insert (bottom) and femoral component (top) each possess three degrees of freedom (DOFs) relative to ground. Tibial insert DOFs are anterior–posterior translation x, medial–lateral translation z, and internal–external rotation β, while femoral component DOFs are superior–inferior translation y, varus–valgus rotation α, and flexion-extension γ. The two components interact via two contacts, one in the $+z$ direction (medial side) and another in the $-z$ direction (lateral side).

outputs, the approach can be easily extended to more complex situations. If more than one contact occurs between a pair of contacting bodies, contact loads for each contact can be fitted separately and then used together during a multibody dynamic simulation. If additional contact model outputs are desired (e.g., contact pressures), these quantities can be calculated and stored during the sampling process and then fitted as a function of the six pose parameters. These extensions will be demonstrated in the practical evaluation described in the following section.

2.3. Surrogate contact model evaluation

We evaluated the accuracy and computational speed of our surrogate contact modeling approach by performing Monte Carlo analyses (i.e., thousands of forward dynamic simulations) using a multibody dynamic model of a cruciate-retaining commercial knee implant (Depuy Orthopedics, Warsaw, IN) mounted in a Stanmore knee wear simulator machine [44]. The goal of the simulations was to predict implant loads, motions, and ultimately wear volume for realistic variations in motion and load inputs to the machine. Symbolic dynamics equations for the model were derived using Kane's method [50] and Autolev (OnLine Dynamics, Sunnyvale, CA). The model possessed six degrees of freedom (DOFs) relative to ground: tibial anterior–posterior translation x, tibial medial–lateral translation z, tibial internal–external rotation β, femoral superior–inferior translation y, femoral varus–valgus rotation α, and femoral flexion–extension γ (Fig. 1). Similar to an actual Stanmore machine, γ was motion controlled, x, y, and β were load controlled, and z and α were left free, where all controlled quantities used ISO standard input curves [45]. Mass properties were estimated from geometric models of the implant and machine components. Soft tissue restraints were simulated by attaching two spring bumpers to the anterior and posterior sides of the tibial component. The springs were attached at the same locations as in the actual simulator machine, and the stiffness of each bi-directional spring was set to 14.48 N/mm for an effective stiffness of 28.96 N/mm [45].

A 3D elastic foundation (EF) contact model [17,46–49] of the knee implant was used to calculate contact loads between the femoral component and tibial insert given the six pose parameters for the contacting bodies. The EF model utilized linear material properties (Young's modulus = 463 MPa, Poisson's ratio = 0.46 [17]) and surface geometry taken from manufacturer computer-aided design models, with contact occurring on the medial and lateral sides of the tibial insert. The EF contact model and symbolic dynamics equations were incorporated into a Matlab program (The Mathworks, Natick, MA) that was used to perform forward dynamic simulations with Matlab's stiff numerical integrator ode15s.

We constructed two surrogate contact models – one for the medial side and another for the lateral side – to replace the elastic foundation contact model within the larger multibody dynamic model. Though a single surrogate contact model would suffice to perform dynamic simulations, two surrogate contact models were needed to calculate wear volume for the medial and lateral sides. To extend our general approach to two contacts between a single pair of bodies using a single set of pose parameters, we replaced the medial and lateral contact loads (i.e., three contact forces and three contact torques per side) with a single set of mechanically equivalent net contact loads. Sensitive directions and sample points were defined using these net contact loads, similar to when only a single contact occurs between a pair of bodies. In contrast, determination and application of the reasonable design space and construction of initial and final surrogate contact models were done for the medial and lateral sides separately.

Below we provide details for how the five-step process described above was implemented to construct medial and lateral surrogate contact models and calculate wear volume on each side.

2.3.1. Step (1): identify sensitive and insensitive directions in the original contact model

To identify sensitive directions, we used a single set of pose parameters to define femoral pose with respect to the tibial insert. With the implant components in a nominal anatomic pose and both sides barely touching, we calculated the sensitivity vector $\mathbf{s}$, as defined in Eq. (1), using net contact loads and identified two sensitive directions. Specifically, net contact force F_y and net contact torque T_α were found to be highly sensitive to small variations in superior–inferior translation y and varus–valgus rotation α, respectively.

2.3.2. Step (2): avoid sample points with undesirable contact load outputs in sensitive directions by changing the definition of a sample point

Given these two sensitive directions, we defined sample points to be combinations of x, F_y, z, T_α, β, γ, where net contact loads F_y and T_α were calculated from the contact loads on the two sides. Thus, during the sampling process, a single sample point definition was used to calculate contact loads on the medial and lateral sides.

2.3.3. Step (3): generate sample point input–output pairs by using design of experiments and repeated static analyses

To generate input–output pairs with the EF contact model, we first determined realistic upper and lower bounds on all pose parameters (one set of six parameters) and contact loads (three sets of six loads – one set each for net, medial, and lateral loads). Initial bounds were extracted from 16 dynamic contact simulations performed with the EF contact model. Motion and net load input curves for the simulations were set to the extremes of their allowable variations for the subsequent Monte Carlo analyses. Based on previous experience [33], we expanded these initial bounds by $p = 50\%$ to define a realistic bounded design space for surrogate contact model creation.

Once these bounds were defined, we used design of experiments and static analyses to develop an initial subset of desirable input–output pairs. While inputs were defined in terms of net contact loads, outputs were defined in terms of medial and lateral contact loads. We first generated $n = 2000$ sample points using the HQ sampling method (Fig. 2a), where the value for n was again chosen based on previous experience [33]. From these 2000 sample points, we then selected the first $m = 500$ points for static analysis with the EF contact model. For each sample point,

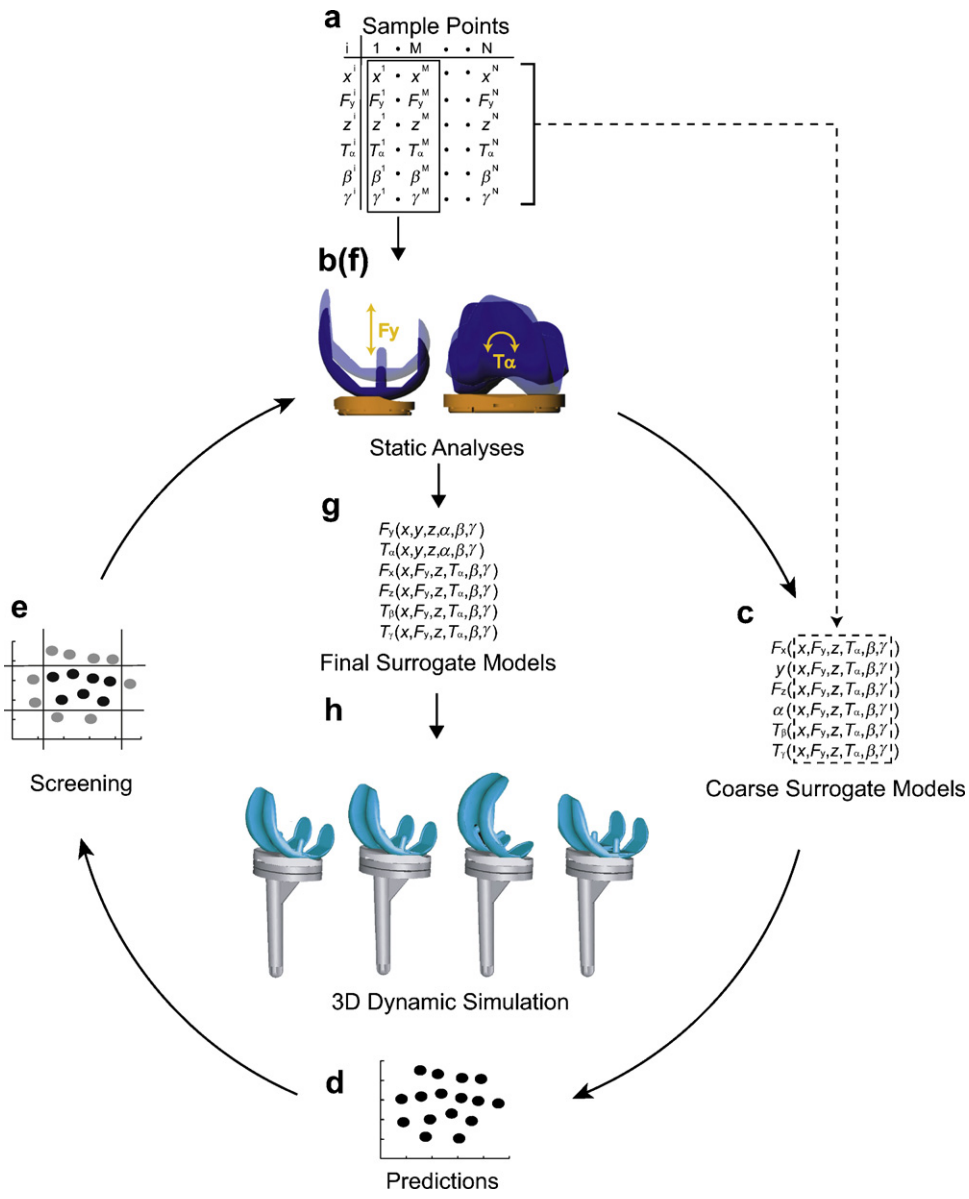

Fig. 2. Overview of the surrogate model creation process. (a) n points are sampled in the x, F_y, z, T_α, β, γ design space. (b) Static analyses are performed for the first m sample points using an elastic foundation (EF) contact model. (c) Coarse surrogate contact models are created based on static analysis results for these m sample points. (d) The coarse surrogate models are used to predict static analysis results for the remaining n–m sample points. (e) Sample points are screened and eliminated if their predicted outputs are outside the desirable ranges defined by one or more nominal EF-based dynamic simulations. (f) Additional static analyses are performed with the EF contact model for sample points that pass the screening process. (g) Final surrogate contact models are created using static analysis results from all retained sample points. (h) During a dynamic simulation, surrogate contact models calculate contact forces and torques applied to the two bodies given the pose of the femoral component relative to the tibial insert.

the static analysis used Matlab's fsolve root-finding algorithm to adjust the sensitive DOFs in the model so as to equilibrate the applied loads with net contact loads calculated from the medial and lateral sides. Each static analysis required approximately 24 s of CPU time on a 3 GHz Pentium IV PC (Fig. 2b). Of the 500 static analyses performed, 18 produced final poses where the net contact loads F_y and T_α were not within 0.1% of the corresponding applied loads. Sample points for these failed static analyses were discarded, leaving 482 sample points for use in the next step.

2.3.4. *Step (4): eliminate sample points with undesirable contact load outputs in insensitive directions by using the concept of a reasonable design space*

To estimate which of the 1500 remaining sample points were within the reasonable design space, we constructed two initial surrogate contact models – one for each side – using the initial 482 desirable sample points. Surrogate model construction was performed using the DACE Kriging Toolbox for Matlab (Fig. 2c; [51]). These two surrogate models were then used to predict EF contact model outputs on the medial and lateral sides for the remaining 1500 sample points (Fig. 2d). Inputs to the two surrogate contact models matched the sample point definition and used net contact loads, while outputs were medial and lateral contact loads. Since outputs from each surrogate contact model corresponded to a static configuration, no static analyses were required for this step, and the specified bounds on medial and lateral contact loads were used to eliminate undesirable sample points. Of the 1500 points analyzed, 934 (937) produced undesirable medial (lateral) outputs, leaving 566 (563) additional sample points to be evaluated with the EF contact model (Fig. 2e).

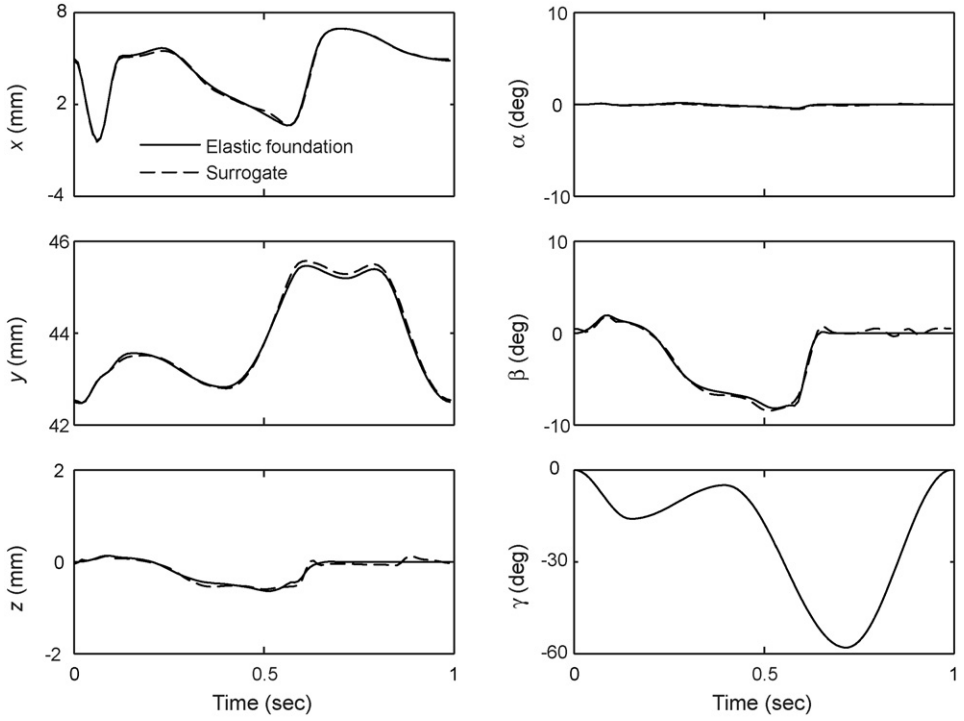

Fig. 3. Comparison of motions predicted by the nominal dynamic simulation performed using the elastic foundation contact model (solid lines) and the surrogate contact models (dashed lines).

2.3.5. Step (5): construct the final surrogate contact model using the desirable subset of the original sample points

After determining the intersection of the desirable sample points for the medial and lateral sides, we performed 560 additional static analyses with the EF contact model (Fig. 2f). The CPU time required for 1060 (=500 + 560) static analyses was approximately 6 h. After eliminating sample points with undesirable medial or lateral outputs, we were left with 982 (=482 + 500) medial and 1042 (=482 + 560) lateral sample points for constructing the final medial and lateral surrogate contact models.

Surrogate model construction for each side required fitting the six contact loads for that side as an explicit or implicit function of the six pose parameters, which were the same for both sides (Fig. 2g):

$$\begin{aligned} F_y &= f(x, y, z, \alpha, \beta, \gamma) \\ T_\alpha &= f(x, y, z, \alpha, \beta, \gamma) \\ F_x &= f(x, F_y, z, T_\alpha, \beta, \gamma) \\ F_z &= f(x, F_y, z, T_\alpha, \beta, \gamma) \\ T_\beta &= f(x, F_y, z, T_\alpha, \beta, \gamma) \\ T_\gamma &= f(x, F_y, z, T_\alpha, \beta, \gamma) \end{aligned} \tag{2}$$

Since $x, y, z, \alpha, \beta, \gamma$ are inputs during a dynamic simulation, contact loads in sensitive directions (i.e., F_y and T_α) were calculated before contact loads in insensitive directions. Thus, for the last four quantities, inputs F_y and T_α were not net loads but rather were the values calculated for the same side. The two final surrogate contact models were composed of two sets of six Kriging models which were incorporated into the multibody dynamic model in place of the EF contact model (Fig. 2h). During a dynamic simulation, net contact loads were generated by combining the outputs of the medial and lateral surrogate contact models.

To calculate medial and lateral wear volume, we created six additional surrogate models to fit medial and lateral center of pressure (CoP) location (three components per side). Each surrogate model took x, F_y, z, T_α, β, γ as inputs, where F_y and T_α were from the side being fitted, and was constructed using the same desirable sample points as the medial and lateral surrogate contact models. The contact force and CoP predictions were then used to calculate medial and lateral wear volume as described previously by Lin et al. [33]. Briefly, Archard's wear law [52] with a wear factor of 1×10^{-7} mm^3/N m [53] was used to calculate one-cycle wear volume on each side from the time history of contact force magnitude and CoP sliding distance. The latter quantity was calculated for each time frame by multiplying the CoP slip speed by the time increment used for numerical integration. CoP slip speed was defined as the magnitude of the CoP velocity in the tibial reference frame, which was calculated from the six pose parameters and their first time derivatives by using rigid body kinematics and treating the CoP as a point fixed in the femoral reference frame [50]. One-cycle wear volume results were extrapolated to 5 million cycles to emulate a typical knee implant wear test [6,19].

To evaluate surrogate contact model accuracy, we performed eleven dynamic wear simulations with the surrogate contact models and the EF contact model used to create them. A nominal dynamic simulation was first performed using the ISO standard input curves and the simulation results from the two models compared quantitatively. Ten additional EF-based and surrogate-based dynamic simulations were then performed to evaluate the extremes in input curve variations used during subsequent Monte Carlo analyses. Specifically, for each of the five Monte Carlo problems described below, we performed two dynamic simulations with each contact model where each input curve represented either a maximum or minimum variation. The ten pairs of results were compared quantitatively by calculating root mean square errors (RMSE) and maximum absolute errors (MAE) for predicted pose parameters, medial and lateral contact loads, and wear volumes. The CoP-based approach for calculating wear volume was also evaluated by calculating wear volume with the EF model using both an element-based approach [18,19] and the CoP-based approach [33].

To evaluate surrogate contact model performance, we performed five Monte Carlo analyses to investigate how realistic variations in motion and load inputs affect predicted wear volume.

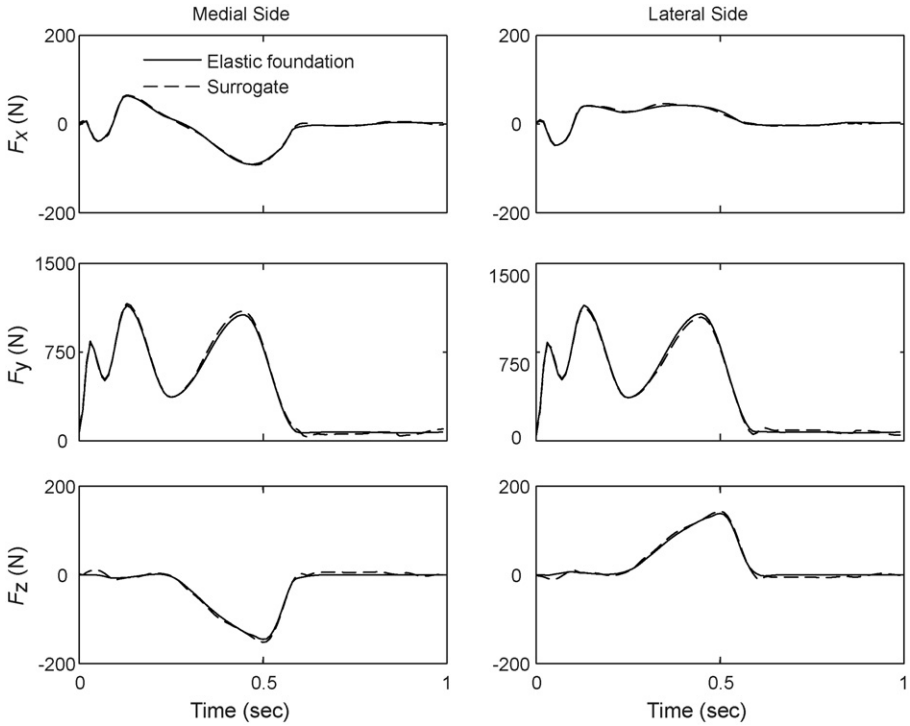

Fig. 4. Comparison of medial and lateral contact forces predicted by the nominal dynamic simulation performed using the elastic foundation contact model (solid lines) and the surrogate contact models (dashed lines).

The first four Monte Carlo analyses varied the three load inputs and one motion input separately while the fifth analysis varied all input profiles together. Principal component analysis was used to create parameterized realistic variations of the input curves based on experimentally observed variations for eight different implant designs tested in a Stanmore simulator machine [33,45]. Each new input curve was generated by selecting weights between 0 and 1 for the first two principal components, which captured 98% of the variability in each type of curve. Each Monte Carlo analysis was performed on a 3 GHz Pentium IV PC and involved at least 1000 forward dynamic simulations utilizing the surrogate contact models. The convergence criterion for each analysis was met when the mean and coefficient of variation (i.e., 100*standard deviation/mean) for the last 10% of the wear predictions were within 2% of the final mean and coefficient of variation [54,55].

3. Results

For the accuracy evaluation, the surrogate-based dynamic simulations closely reproduced the contact kinematics, contact loads, and wear volumes predicted by the EF-based dynamic simulations (Figs. 3–5). On average, the RMSE and MAE for the 3D translations/rotations were less than 0.2 mm/0.6° and 0.3 mm/1.3°, respectively. For the medial contact forces/torques, RMSE and MAE were less than 20 N/0.54 N m and 46 N/1.1 N m, respectively, while for the lateral contact forces/torques, they were less than 20 N/0.56 N m and 41 N/1.1 N m, respectively. For both the surrogate-based and EF-based dynamic simulations, the CoP-based approach for predicting wear volume reproduced the element-based EF results to within 2% error (Table 1).

For the performance evaluation, surrogate-based dynamic simulations were significantly faster than EF-based dynamic simulations. Each forward dynamic simulation performed during a Monte Carlo analysis required approximately 5 s of CPU time, whereas a single simulation performed with the EF contact model required 17 min. Total CPU time to complete one Monte Carlo analysis was 1.4 h (excluding the 6 h required for surrogate model creation) compared to an estimated 284 h (11.8 days) with the EF contact model. The Monte Carlo analyses revealed that wear volume was more sensitive to realistic changes in input motion than to realistic changes in input loads (Fig. 6). While 10th to 90th percentile wear volume spanned at most 3 mm^3 when each input load was changed separately, it spanned 12 mm^3 when only the input motion was changed. When input motion and loads were changed simultaneously, the span was increased to 20 mm^3, indicating an interactive effect.

4. Discussion

This paper presented a novel method for performing computationally efficient elastic contact analyses within multibody dynamic simulations. The method is derived from surrogate modeling con-

Table 1
Comparison of wear volumes (mm^3) predicted by dynamic simulations performed using the elastic foundation contact model and the surrogate contact model with load and motion input curves varied to the extremes used in the Monte Carlo analyses.

Quantity	Variation	Elastic foundation contact model	Surrogate contact model	Difference (%)
F_x		28.44	28.51	0.24
F_y		30.31	30.27	0.14
T_β	Maximum	18.14	18.24	0.56
γ		17.10	17.23	0.72
All		29.76	29.52	0.80
F_x		29.49	29.20	1.02
F_y		30.19	29.73	1.53
T_β	Minimum	27.63	27.37	0.96
γ		27.08	26.90	0.66
All		30.11	30.08	0.10

F_x, F_y, T_β, and γ are defined based on the generalized coordinates in Fig. 1.

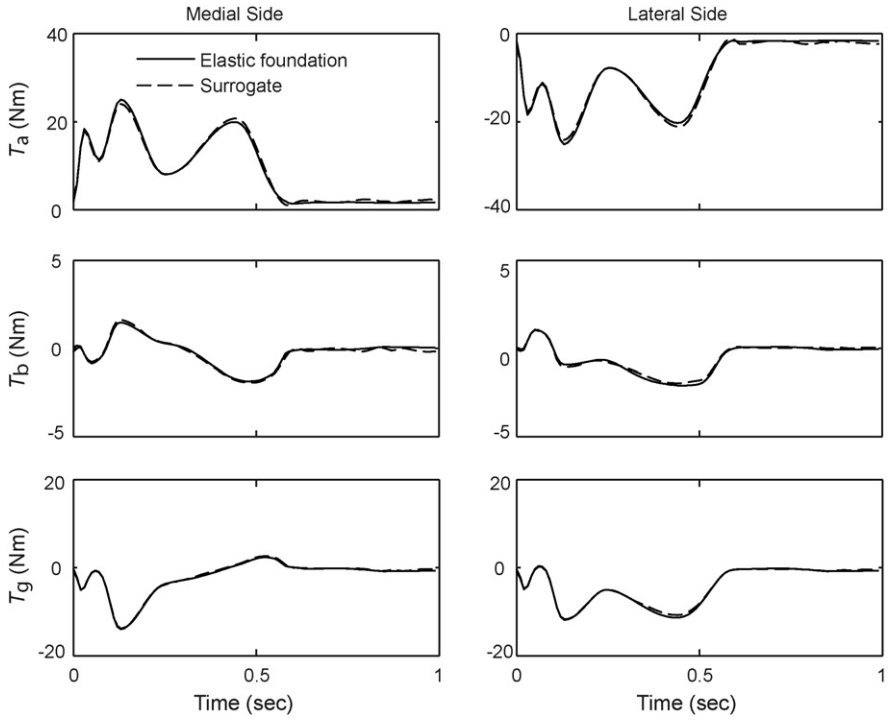

Fig. 5. Comparison of medial and lateral contact torques predicted by the nominal dynamic simulation performed using the elastic foundation contact model (solid lines) and the surrogate contact models (dashed lines).

cepts and has the greatest potential value for applications requiring repeated simulations, such as sensitivity and optimization studies. Surrogate contact models can be fitted to input–output relationships sampled from any elastic contact model (e.g., finite element, elastic foundation) once sensitive directions have been identified. The computational cost of using a surrogate contact model is paid up front when sampling the original contact model via repeated static analysis. Thereafter, computational cost is low since repeated geometry evaluations and solution of linear or nonlinear systems of equations are eliminated. The methodology was successfully applied to dynamic wear simulation of a commercial knee implant tested in a Stanmore knee simulator machine. Dynamic simulations performed with the surrogate contact models were highly accurate compared to simulations performed with the elastic foundation contact model used to create the surrogates. Even including the 6 h of CPU time required for surrogate model creation, CPU time required to perform five Monte Carlo analyses (approximately 13 h) was over 100 times less than if an elastic foundation contact model has been used (approximately 1420 h).

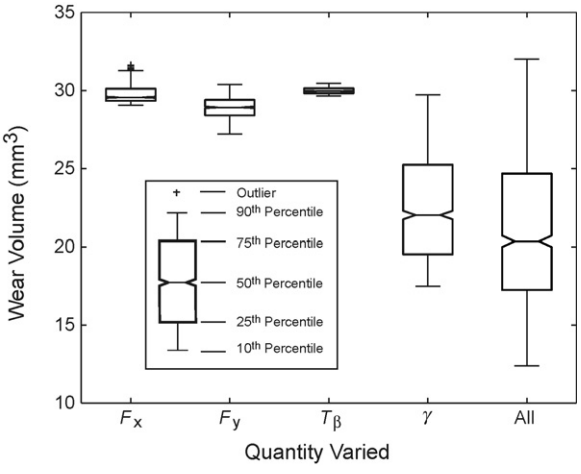

Fig. 6. Box plot distributions of wear volume predicted by five Monte Carlo analyses performed using repeated dynamic simulations with the surrogate contact models. Simulator machine inputs varied by the analyses were anterior–posterior force applied to the tibial insert (F_x), superior–inferior force applied to the femoral component (F_y), internal–external torque applied to the tibial insert (T_β), and flexion–extension motion applied to the femoral component (γ).

Despite its computational benefits, our proposed surrogate contact modeling method possesses at least five important limitations. First, determination of sensitive directions is influenced by how coordinate systems are embedded in the master and slave bodies. For instance, contact force F_y would become sensitive to changes in X translation as well as to changes in Y translation if the tibial insert coordinate system was rotated relative to the insert geometry by 45° about its Z axis. This situation would create unnecessary coupling between these two directions. To minimize coupling, principal component analysis could be used to determine "principal sensitive directions." Alternatively, for some geometries, it may be possible to perform all sampling in force/torque space and then either swap all contact model outputs and inputs or solve a six-dimensional root-finding problem for the fitting process. Further research is required to determine the best way to address potential coupling effects.

Second, for some geometries, sensitive directions could change with model pose. One possibility for addressing this issue would be to allow for different sample point definitions in different regions of design space. Consider a direction that was initially treated as insensitive, meaning that poses for that direction were used to define sample points. With the current "reasonable design space" approach, if a contact force or torque outside the allowable bounds was encountered for that direction, we would simply delete that sample point. However, if we wanted to account for the possibility that we had encountered a region of design space where this direction had become sensitive, we could switch from sampling a single pose value to sampling a series of load values for that one sample point.

A third limitation is that a new surrogate contact model must be generated any time the geometries or material properties of the

contacting bodies are changed. This limitation is not serious for the current application since recent studies have reported that predicted wear volume (but not wear area and depth) is relatively insensitive to whether or not the surface geometry is changed progressively over a sequence of wear simulations [6,19]. Furthermore, this limitation could be overcome by employing geometric or material parameter values as additional sampled inputs during the surrogate model creation process. For geometric changes, a parametric CAD program could be used to create the necessary geometry for each combination of geometry parameter inputs [31]. For material property changes, a parametric material model could be used to define linear or nonlinear material properties for each combination of material parameter inputs [32]. In both cases, one would want the number of new input parameters to be as low as possible to keep the surrogate contact model fitting process as simple as possible.

A fourth limitation is that evaluation of surrogate contact model accuracy currently requires performing the same dynamic simulation with the computationally expensive contact model. A method is needed for evaluating the surrogate contact model by itself apart from a dynamic simulation. Standard surrogate model evaluation methods exist, such as calculating errors at additional sample points not used for surrogate model creation or performing prediction error sum of squares analysis using the original sample points [56]. However, it is difficult to correlate the errors measured by different evaluation methods with whether or not an accurate dynamic simulation can be completed with the surrogate contact model. One possible alternative is to perform a probabilistic analysis of the pose parameter combinations likely to be encountered during a dynamic simulation. Such an analysis could establish measures for whether or not a sample point has a high likelihood of being encountered. Requiring all sample points to have a high likelihood would provide greater confidence that the surrogate model will produce accurate dynamic simulation results.

A fifth limitation is that the current methodology does not account for friction forces between the contacting surfaces. However, it should not be difficult to add a Coulomb friction model to a surrogate contact model. This comment is based on our success, both in the current study and a previous one [33], creating surrogate models to predict CoP location and ultimately wear volume accurately. Required inputs to our CoP-based wear volume calculation are the net normal contact force applied at the CoP and the slip velocity at the CoP – the same two inputs required for a Coulomb friction model. Thus, at each instant in time during a forward dynamic simulation, it would not be difficult to calculate a Coulomb friction force to be applied at the CoP. The friction force at the current time instant would then affect the model pose at future time instants.

The reasonableness of using coarse surrogate contact models to filter out undesirable sample points depends on the accuracy of the filtering process. The coarse surrogate models may have identified some desirable points as undesirable and vice versa. To investigate this possibility, we performed a static analysis with the EF contact model for each of the 1500 sample points filtered using the course surrogate contact models. We found that 5% of the sample points identified as undesirable turned out to be within the reasonable design space. For sample points identified as desirable, we found that 88% were actually desirable. Thus, while the reasonable design space filtering process was not perfect, it was highly effective at identifying desirable and undesirable sample points before evaluation with the original contact model. If computation time for sample point evaluation is not of concern, then this filtering step could be omitted and all sample points could be evaluated using the original contact model.

Theoretically, three different fitting methods could be used to develop a surrogate contact model. The first method is consistent with how a surrogate contact model is used during a dynamic simulation, where it functions like a nonlinear spring. This method uses the six pose parameters as inputs and calculates the six contact loads as outputs. The second method is consistent with how the original surrogate contact model is used during sampling via repeated static analyses, where sensitive directions are important. This method uses the two contact loads in sensitive directions and four pose parameters in insensitive directions as inputs and calculates the two pose parameters in sensitive directions and four contact loads in insensitive directions as outputs. The third method is a hybrid of the first two. It calculates contact loads in the two sensitive directions (i.e., F_y and T_x) using the first method and contact loads in the remaining directions using the second method. While the first method is the most direct, it produces less accurate dynamic simulation results than does the hybrid method, possibly because of small fitting errors in the sensitive directions. The drawback of the second method is that a two-dimensional root-finding problem must be solved to determine F_y and T_x given the input values of y and α, making the method less appealing in practice. In our experience, the hybrid method has provided the best accuracy with the minimum amount of computational cost.

While this study has demonstrated that surrogate contact models can be beneficial for sensitivity studies, the greatest computational benefit is likely to occur for optimization studies. For stochastic sensitivity studies of wear in knee replacements, the mean value method [57] has successfully reproduced Monte Carlo wear predictions in only 6% of the computation time, primarily by reducing the number of simulations [58]. In contrast, few good methods exist for reducing the number of simulations in optimization studies. For gradient-based optimizations, automatic differentiation (AD) can be used to replace repeated simulations required for finite-difference derivatives. Though AD cannot be used with traditional elastic contact models, it can theoretically be applied to surrogate contact models, since the input–output relationships are described by analytic functions. Surrogate contact models can also reduce computation time per simulation if finite-difference derivatives are used. For example, surrogate contact models recently facilitated simultaneous estimation of muscle and contact forces in the knee during gait using gradient-based optimization with finite-difference derivatives [59]. While optimization of a complete gait cycle required approximately 32 h of CPU time using EF contact models, the same optimization required only 42 min of CPU time using surrogate contact models.

On a practical basis, the sensitivity analysis results demonstrated the importance of closely controlling knee simulator machine inputs, especially femoral flexion angle. When small variations were imposed on the input motion and loads, variations in the femoral flexion angle had the largest influence on predicted wear volume (Fig. 6). This finding is consistent with two previous studies that performed probabilistic analyses of knee replacement wear in a Stanmore simulator machine [33,58].

In summary, this paper has presented a surrogate contact modeling method that can significantly improve the computational speed of three-dimensional multibody dynamic simulations. The accuracy and performance of the method were evaluated using a combination of dynamic simulations and Monte Carlo analyses. The approach has the potential to facilitate sensitivity and optimization studies of multibody dynamic systems incorporating elastic contact models, such as musculoskeletal models incorporating joint contact models, and it may also provide a computationally efficient means for contact detection within such systems.

Acknowledgments

This work was supported by the National Science Foundation CBET Division under Grant No. 0602996 to B.J.F. and R.T.H. and CAREER Award No. 0239042 to B.J.F.

Conflict of interest statement

The authors have no conflict of interest.

References

[1] Schiehlen W, Guse N, Seifried R. Multibody dynamics in computational mechanics and engineering applications. Computer Methods in Applied Mechanics and Engineering 2006;195:5509–22.
[2] Sharf I, Zhang YN. A contact force solution for non-colliding contact dynamics simulation. Multibody System Dynamics 2006;16:263–90.
[3] Glocker C. Formulation of spatial contact situations in rigid multibody systems. Computer Methods in Applied Mechanics and Engineering 1999;177:199–214.
[4] Cheng RC-K, Brown TD, Andrews JG. Non-uniqueness of the bicompartmental contact force solution in a lumped parameter mathematical model of the knee. Journal of Biomechanics 1990;23:353–5.
[5] Halloran JP, Easley SK, Petrella AJ, Rullkoetter PJ. Comparison of deformable and elastic foundation finite element simulations for predicting knee replacement mechanics. Journal of Biomechanical Engineering 2005;127:813–8.
[6] Knight LA, Pal S, Coleman JC, Bronson F, Haider H, Levine DL, et al. Comparison of long-term numerical and experimental total knee replacement wear during simulated gait loading. Journal of Biomechanics 2007;40:1550–8.
[7] Lanovaz JL, Ellis RE. A cadaverically evaluated dynamic FEM model of closed-chain TKR mechanics. Journal of Biomechanical Engineering 2009;131:051002.
[8] Halloran JP, Petrella AJ, Rullkoetter PJ. Explicit finite element modeling of total knee replacement mechanics. Journal of Biomechanics 2005;38:323–31.
[9] Godest AC, Beaugonin M, Haug E, Taylor M, Gregson PJ. Simulation of a knee joint replacement during a gait cycle using explicit finite element analysis. Journal of Biomechanics 2002;35:267–75.
[10] Lanovaz JL, Ellis RE. Dynamic simulation of a displacement-controlled total knee replacement wear tester. Proceedings of the Institution of Mechanical Engineers, Part H: Journal of Engineering in Medicine 2008;222:669–81.
[11] D'Lima DD, Steklov N, Fregly BJ, Banks SA, Colwell Jr CW. In vivo contact stresses during activities of daily living after knee arthroplasty. Journal of Orthopaedic Research 2008;26:1549–55.
[12] Donahue TL, Hull ML, Rashid MM, Jacobs CR. A finite element model of the human knee joint for the study of tibio-femoral contact. Journal of Biomechanical Engineering 2002;124:273–80.
[13] Sarathi Kopparti P, Lewis G. Influence of three variables on the stresses in a three-dimensional model of a proximal tibia-total knee implant construct. Biomedical Materials and Engineering 2007;17:19–28.
[14] Rawlinson JJ, Furman BD, Li S, Wright TM, Bartel DL. Retrieval, experimental, and computational assessment of the performance of total knee replacements. Journal of Orthopaedic Research 2006;24:1384–94.
[15] Knight LA, Pal S, Coleman JC, Bronson F, Haider H, Levine DL, et al. Comparison of long-term numerical and experimental total knee replacement wear during simulated gait loading. Journal of Biomechanics 2007;40:1550–8.
[16] Bei Y, Fregly BJ. Multibody dynamic simulation of knee contact mechanics. Medical Engineering & Physics 2004;26:777–89.
[17] Fregly BJ, Bei Y, Sylvester ME. Experimental evaluation of an elastic foundation model to predict contact pressures in knee replacements. Journal of Biomechanics 2003;36:1659–68.
[18] Fregly BJ, Sawyer WG, Harman MK, Banks SA. Computational wear prediction of a total knee replacement from in vivo kinematics. Journal of Biomechanics 2005;38:305–14.
[19] Zhao D, Sadoka H, Sawyer WG, Banks SA, Fregly BJ. Predicting knee replacement damage in a simulator machine using a computational model with a consistent wear factor. Journal of Biomechanical Engineering 2008;130, 011004.
[20] Landon RL, Hast MW, Piazza SJ. Robust contact modeling using trimmed NURBS surfaces for dynamic simulations of articular contact. Computer Methods in Applied Mechanics and Engineering 2009;198:2339–46.
[21] Moran MF, Bhimji S, Racanelli J, Piazza SJ. Computational assessment of constraint in total knee replacement. Journal of Biomechanics 2008;41:2013–20.
[22] Strickland MA, Taylor M. In-silico wear prediction for knee replacements—methodology and corroboration. Journal of Biomechanics 2009;42:1469–74.
[23] Cox SE, Haftka RT, Baker CA, Grossman B, Mason WH, Watson LT. A comparison of global optimization methods for the design of a high-speed civil transport. Journal of Global Optimization 2001;21:415–33.
[24] Farhang-Mehr A, Azarm S. Bayesian meta-modelling of engineering design simulations: a sequential approach with adaptation to irregularities in the response behaviour. International Journal for Numerical Methods in Engineering 2005;62:2104–26.
[25] Liu B, Haftka RT, Akgun MA. Two-level composite wing structural optimization using response surfaces. Structural and Multidisciplinary Optimization 2000;20:87–96.
[26] Queipo NV, Pintos S, Rincon N, Contreras N, Colmenares J. Surrogate modeling-based optimization for the integration of static and dynamic data into a reservoir description. Journal of Petroleum Science and Engineering 2002;35:167–81.
[27] Roux WJ, Stander N, Haftka RT. Response surface approximations for structural optimization. International Journal for Numerical Methods in Engineering 1998;42:517–34.
[28] Wang GG, Shan S. Review of metamodeling techniques in support of engineering design optimization. Journal of Mechanical Design 2007;129:370–80.
[29] Xiong Y, Chen W, Apley D, Ding X. A non-stationary covariance-based Kriging method for metamodelling in engineering design. International Journal for Numerical Methods in Engineering 2007;71:733–56.
[30] Bouzid AH, de Technologie Superieure E, Champliaud H. On the use of dual Kriging interpolation for the evaluation of the gasket stress distribution in bolted joints. In: Proceedings of the ASME pressure vessels and piping conference. 1998.
[31] Chang PB, Williams BJ, Santner TJ, Notz WI, Bartel DL. Robust optimization of total joint replacements incorporating environmental variables. Journal of Biomechanical Engineering 1999;121:304–10.
[32] Lin YC, Farr J, Carter K, Fregly BJ. Response surface optimization for joint contact model evaluation. Journal of Applied Biomechanics 2006;22:120–30.
[33] Lin YC, Haftka RT, Queipo NV, Fregly BJ. Two-dimensional surrogate contact modeling for computationally efficient dynamic simulation of total knee replacements. Journal of Biomechanical Engineering 2009;131:041010.
[34] Halloran JP, Erdemir A, van den Bogert AJ. Adaptive surrogate modeling for efficient coupling of musculoskeletal control and tissue deformation models. Journal of Biomechanical Engineering 2009;131:011014.
[35] McKay MD, Beckman RJ, Conover WJ. A comparison of three methods for selecting values of input variables in the analysis of output from a computer code. Technometrics 2000;42:55–61.
[36] Hammersley JM. Monte Carlo methods for solving multivariable problems. Annals of the New York Academy of Sciences 1960;86:844–74.
[37] Myers RH, Montgomery DC. Response surface methodology: process and product in optimization using designed experiments. New York: John Wiley and Sons Inc.; 1995.
[38] Diwekar UM. Introduction to applied optimization. Springer; 2003.
[39] Kalagnanam JR, Diwekar UM. An efficient sampling technique for off-line quality control. Technometrics 1997;39:308–19.
[40] Hosder S, Watson LT, Grossman B, Mason WH, Kim H, Haftka RT, et al. Polynomial response surface approximations for the multidisciplinary design optimization of a high speed civil transport. Optimization and Engineering 2001;22:431–52.
[41] Kaufman MD, Balabanov V, Burgee SL, Giunta AA, Grossman B, Haftka RT, et al. Variable-complexity response surface approximations for wing structural weight in HSCT design. Computational Mechanics 1996;18:112–26.
[42] Mack Y, Goel T, Shyy W, Haftka RT. Surrogate model-based optimization framework: a case study in aerospace design. Studies in Computational Intelligence 2007;51:323–42.
[43] Krige DG. A statistical approach to some mine valuations and allied problems at the Witwatersrand. University of Witwatersrand; 1951.
[44] Walker PS, Blunn GW, Broome DR, Perry J, Watkins A, Sathasivam S, et al. A knee simulating machine for performance evaluation of total knee replacements. Journal of Biomechanics 1997;30:83–9.
[45] DesJardins JD, Walker PS, Haider H, Perry J. The use of a force-controlled dynamic knee simulator to quantify the mechanical performance of total knee replacement designs during functional activity. Journal of Biomechanics 2000;33:1231–42.
[46] An KN, Himenso S, Tsumura H, Kawai T, Chao EYS. Pressure distribution on articular surfaces: application to joint stability analysis. Journal of Biomechanics 1990;23:1013–20.
[47] Blankevoort L, Kuiper JH, Huiskes R, Grootenboer HJ. Articular contact in a three-dimensional model of the knee. Journal of Biomechanics 1991;24:1019–31.
[48] Li GA, Sakamoto M, Chao EYS. A comparison of different methods in predicting static pressure distribution in articulating joints. Journal of Biomechanics 1997;30:635–8.
[49] Pandy MG, Sasaki K, Kim S. A three-dimensional musculoskeletal model of the human knee joint. Part 1: Theoretical construct. Computer Methods in Biomechanics and Biomedical Engineering 1998;1:87–108.
[50] Kane TR, Levinson DA. Dynamics, theory and applications. New York: McGraw-Hill; 1985.
[51] Lophaven SN, Nielsen HB, Sundergaard J. DACE-A Matlab Kriging toolbox; 2002.
[52] Archard JF, Hirst W. The wear of metals under unlubricated conditions. In: Proceedings of the Royal Society of London Series A—Mathematical and physical sciences. 1956.
[53] Fisher J, Dowson D, Hamdzah H, Lee HL. The effect of sliding velocity on the friction and wear of UHMWPE for use in total artificial joints. Wear 1994;175:219–25.
[54] Fishman GS. Monte Carlo: concepts, algorithms and applications. Springer; 1996.
[55] Valero-Cuevas FJ, Johanson ME, Towles JD. Towards a realistic biomechanical model of the thumb: the choice of kinematic description may be more critical than the solution method or the variability/uncertainty of musculoskeletal parameters. Journal of Biomechanics 2003;36:1019–30.

[56] Martens H, Naes T. Multivariate calibration. New York: John Wiley and Sons Inc.; 1984.
[57] Wu YT, Millwater HR, Cruse TA. Advanced probabilistic structural-analysis method for implicit performance functions. AIAA Journal 1990;28:1663–9.
[58] Pal S, Haider H, Laz PJ, Knight LA, Rullkoetter PJ. Probabilistic computational modeling of total knee replacement wear. Wear 2008;264:701–7.
[59] Lin YC, Walter JP, Banks SA, Pandy MG, Fregly BJ. Simultaneous prediction of muscle and contact forces in the knee during gait. Journal of Biomechanics 2010;43:945–52.